Available online at www.sciencedirect.com
SCIENCE DIRECT®
Journal of Solid State Chemistry 177 (2004) 2423–2431
JOURNAL OF SOLID STATE CHEMISTRY
http://elsevier.com/locate/jssc

Synthesis of new molybdenum–tungsten, vanadium–tungsten and vanadium–molybdenum–tungsten oxynitrides from freeze-dried precursors

Abdelouahad El-Himri,[a,b] Pedro Núñez,[a,*] Fernando Sapiña,[b] Rafael Ibáñez,[b] Aurelio Beltrán,[b] and José-María Martínez-Agudo[c]

[a] *Departamento de Química Inorgánica, Universidad de La Laguna, Avda. Astrofisico Fco. Sanchez, 38200 La Laguna, Tenerife, Canary Islands, Spain*
[b] *Institut de Ciència dels Materials de la Universitat de València, Apartado de Correos 2085, E-46071 València, Spain*
[c] *Departamento de Química Inorgánica, Institut de Ciéncia Molecular, Universidad de Valencia, Dr. Moliner 50, 46100 Burjassot, Spain*

Received 2 March 2004; received in revised form 20 March 2004; accepted 4 April 2004

Abstract

Interstitial molybdenum–tungsten, vanadium–tungsten and vanadium–molybdenum–tungsten oxynitrides in the solid solution series $Mo_{1-z}W_z(O_xN_y)$ and $V_{1-z}W_z(O_xN_y)$ ($z = 0$, 0.2, 0.4, 0.5, 0.6, 0.8, 1), and $V_{1-u-z}Mo_uW_z(O_xN_y)$ (u, $z = 0.2$, 0.33, 0.4, 0.6; $u + z < 1$), have been obtained by ammonolysis of precursors resulting from the freeze-drying of aqueous solutions of the metal salts (NH_4VO_3, $(NH_4)_6Mo_7O_{24} \cdot 4H_2O$ and $(NH_4)_6W_{12}O_{39} \cdot 18H_2O$). A study of the influence of the preparative variables on the outcomes of this procedure is presented. Compounds in the $Mo_{1-z}W_z(O_xN_y)$ series are prepared as single phases by ammonolysis of the respective freeze-dried precursors (during 2 h) at different temperatures between 973 and 1023 K, optimised for each composition, followed by slow cooling of the samples (except for the Mo-only containing phase, in which fast cooling has been used). Compounds in the $V_{1-z}W_z(O_xN_y)$ and $V_{1-u-z}Mo_uW_z(O_xN_y)$ series are prepared as single phases by ammonolysis (during 2 h) of crystalline precursors (as resulting from thermal treatment in air at 873 K, during 12 h, of the freeze-dried precursors) at 1073 K, followed by slow cooling of the samples. All the compounds in these series have the rock-salt crystal structure, in which the metal atoms are in an fcc arrangement, with non-metal atoms occupying octahedral interstitial positions. The materials have been characterized by X-ray powder diffraction, elemental analysis, scanning electron microscopy and magnetic measurements.

Keywords: Nitride; Oxynitride; Freeze dried; Precursor; Ammonolysis; Materials; Molybdenum; Tungsten; Vanadium

1. Introduction

Transition-metal nitrides have attracted attention mainly because they exhibit technologically important properties [1]. In fact, some of them have been compared to noble metals, basis on their unusual features related to properties like hardness, thermal and electrical conductivity or catalytic performances [2]. While monometallic nitrides have widely been investigated long time ago [3], progress in nitride chemistry beyond binary systems was limited until around the middle of the decade of 1980 due to preparative difficulties [4,5]. Research in this area is currently growing as more applications for these materials arise [6]. In a previous publication [7], we referred to the implementation of new preparation techniques in recent years as the essential basis on which the list of new polymetallic nitrides and oxynitrides is readily increasing.

A common feature of the new synthetic methodologies is the search for alternative reaction paths through which the cationic diffusion distances become lowered, which would enable nitride preparation at relatively low temperatures [5,7]. The use of bimetallic mixed oxide precursors [8] and the nitridation of metallorganic hydroxide [9] are two of the most successful among these approaches, even though they have limitations which have been discussed elsewhere [7]. In this context, the use of precursors obtained by freeze-drying of aqueous solutions of the appropriate metal salts has

*Corresponding author. Fax: +34922318464.
E-mail address: pnunez@ull.es (P. Núñez).

0022-4596/$ - see front matter © 2004 Elsevier Inc. All rights reserved.
doi:10.1016/j.jssc.2004.04.010

proved to be a very versatile soft method for obtaining stoichiometrically controlled complex polymetallic systems (from high T_c superconducting materials [10] to polymetallic nitrides and oxynitrides [11] intermetallics [12], among other materials). In practice, dealing with complex nitrides, ammonolysis processes (under relatively mild conditions) of freeze-dried precursors has enabled us the preparation of Ni_2Mo_3N [7] and Pd_2Mo_3N [11] together with a diversity of compositions in the solid solution series $V_{1-z}Mo_z(O_xN_y)$ [13], $V_{1-z}Cr_z(O_xN_y)$ and $Cr_{1-z}Mo_z(O_xN_y)$ [14].

Besides their unusual properties, Mo or W containing carbides, nitrides and oxynityrides have proved to be very efficient catalysts in different relevant processes [1,15], including hydrodenitrogenation [16] and ammonia synthesis [17]. To expand possibilities, we have explored the opportunity of applying our synthetic methodology to the synthesis of new polymetallic Mo and/or W-containing nitrides and oxynitrides. Here, we report on how the use of freeze-dried polymetallic precursors has allowed us to prepare oxynitrides in different new solid solution series, $Mo_{1-z}W_z(O_xN_y)$ and $V_{1-z}W_z(O_xN_y)$ ($z = 0$, 0.2, 0.4, 0.5, 0.6, 0.8, 1), and $V_{1-u-z}Mo_uW_z(O_xN_y)$ (u, $z = 0.2$, 0.33, 0.4, 0.6, $u + z < 1$).

2. Experimental

2.1. Synthesis

Materials used as reagents in the current investigation were NH_4VO_3 (Fluka, 99.0%), $(NH_4)_6Mo_7O_{24}\cdot 4H_2O$ (Panreac, 99.0%) and $(NH_4)_6W_{12}O_{39}\cdot 18H_2O$ (Aldrich, 99.98%). Starting V, Mo or W containing solutions were prepared by dissolving their respective salts in distilled water. Then, they were combined to obtain Mo–W, V–W and V–Mo–W source solutions whose total cationic concentrations were 0.50 M, and molar nominal compositions Mo:W or V:W = $1-z$:z ($z = 0$, 0.2, 0.4, 0.5, 0.6, 0.8, 1), and V:Mo:W = $1-u-z$:u:z (u, $z = 0.2$, 0.33, 0.4, 0.6, $u + z < 1$). The amounts of the different reagents were adjusted to give 5 g of the final products. Droplets of these solutions were flash frozen by projection on liquid nitrogen and then freeze-dried at a pressure of 1–10 Pa in a Labconco freeze drier. In this way, dried solid precursors were obtained as amorphous (X-ray diffraction) loose powders. Crystalline precursors for the V–W and V–Mo–W series were obtained by heating the amorphous freeze-dried precursor for 12 h under air at 873 K.

Mo–W, V–W and V–Mo–W oxynitrides were synthesized by ammonolysis of the adequate precursors, amorphous or crystalline. The gases employed in the ammonolysis process were NH_3 (99.9%) and N_2 (99.9995%). A sample of the selected crystalline precursor (ca. 0.5 g) was placed into an alumina boat, which was then inserted into a quartz flow-through tube furnace. The gas output of the tube furnace was connected to an acetic acid trap and the input was connected to the gas line. Prior to initiate the thermal treatment, the tube furnace was purged for 15 min with N_2 and another 15 min with NH_3. Several runs under different experimental conditions were also performed in order to determine the appropriate conditions for the preparation of pure samples. The precursor powder was heated at 5 K min^{-1} to a final temperature (T_f) that was held for a period of time (t_{hold}) under flowing ammonia (50 cm^3 min^{-1}). Then, the solid was cooled down at different variable rates (r_c) in the same atmosphere. The different cooling rates were obtained by either turning off the oven leaving the sample inside (slow cooling, ca. 4 K min^{-1}) or by quenching at room temperature (fast cooling, ca. 50 K min^{-1}). After cooling, the products were always passivated with flowing nitrogen for 20 min. All products were stored in a desiccator over $CaCl_2$.

2.2. Characterization

2.2.1. Elemental analysis

Metal ratios in the solids were determined by energy dispersive analysis of X-ray (EDAX) on a Jeol JSM 6300 scanning electron microscope, that were collected by an Oxford detector with quantification performed using virtual standards on associated Link-Isis software. The operating voltage was 20 kV, and the energy range of the analysis 0–20 keV. The nitrogen content of the oxynitrides was evaluated by standard combustion analysis (EA 1108 CHNS-O); N_2 and CO were separated in a chromatographic column, and measured using a thermal conductivity detector. The oxygen content was indirectly determined by thermogravimetric analysis (Perkin-Elmer TGA 7 system). Indeed, the samples were heated under oxygen until complete oxidation (5 K min^{-1} up to T_{final} ca. 773–873 K, these temperatures being well below the sublimation temperatures of the corresponding oxides). The final products were determined by means of X-ray powder diffraction experiments. The oxygen content was estimated from the observed weight increase, taking into account the nature of the final phases. Summarized in Tables 1–3 are the results of these analyses for the resulting oxynitrides. As shown by EDAX, the freeze-dried precursors are homogeneous at micron scale.

2.2.2. X-ray diffraction

X-ray powder diffraction patterns were obtained from a Phillips X'pert automated diffractometer using graphite-monochromated Cu$K\alpha$ radiation. Samples were dusted through a sieve on the holder surface. Routine patterns for phase identification were collected with a scanning step of 0.08° in 2θ over the angular range

Table 1
Chemical composition, cell parameters and crystallite size of molybdenum tungsten oxynitrides $Mo_{1-z}W_z(O_xN_y)$

z	z (EDAX)	Oxygen (wt%)	Nitrogen (wt%)	Proposed stoichiometry	t (nm)	Cell parameter, a (Å)
0.0	—	6.8(5)	7.3(3)	$Mo(O_{0.47}N_{0.58})$	6	4.1819 (2)
0.2	0.19	1.9(1)	11.5(4)	$Mo_{0.8}W_{0.2}(O_{0.15}N_{1.08})$	4	4.11581 (12)
0.4	0.40	1.6(1)	10.0(3)	$Mo_{0.6}W_{0.4}(O_{0.25}N_{1.08})$	5	4.11722 (11)
0.5	0.51	3.5(3)	7.1(3)	$Mo_{0.5}W_{0.5}(O_{0.34}N_{0.79})$	4	4.10836 (11)
0.6	0.60	2.0(2)	7.4(3)	$Mo_{0.4}W_{0.6}(O_{0.21}N_{0.87})$	5	4.11385 (13)
0.8	0.81	4.5(4)	7.4(3)	$Mo_{0.2}W_{0.8}(O_{0.55}N_{0.99})$	5	4.08268 (13)
1.0	—	2.0(2)	5.9(3)	$W(O_{0.25}N_{0.78})$	5	4.1253 (6)

Table 2
Chemical composition, cell parameters and crystallite size of vanadium tungsten oxynitrides, $V_{1-z}W_z(O_xN_y)$

z	z (EDAX)	Oxygen (wt%)	Nitrogen (wt%)	Proposed stoichiometry	t (nm)	Cell Parameter, a (Å)
0.0	—	4.6(3)	12.4(4)	$V(O_{0.18}N_{0.54})$	25	4.1055 (4)
0.2	0.21	3.4(3)	13.9(4)	$V_{0.8}W_{0.2}(O_{0.2}N_{0.93})$	10	4.1173 (7)
0.4	0.41	1.9(2)	10.5(4)	$V_{0.6}W_{0.4}(O_{0.14}N_{0.89})$	10	4.1207 (8)
0.5	0.51	2.4(2)	9.2(3)	$V_{0.5}W_{0.5}(O_{0.2}N_{0.87})$	10	4.1280 (4)
0.6	0.62	2.4(2)	8.6(3)	$V_{0.4}W_{0.6}(O_{0.22}N_{0.9})$	10	4.1305 (4)
0.8	0.8	4.0(3)	7.2(3)	$V_{0.2}W_{0.8}(O_{0.44}N_{0.91})$	10	4.1333 (2)
1.0	—	2.2(2)	6.1(3)	$W(O_{0.27}N_{0.87})$	6	4.1325 (3)

Table 3
Chemical composition, cell parameters and crystallite size of vanadium molybdenum tungsten oxynitrides, $V_{1-u-z}Mo_uW_z(O_xN_y)$

$1-u-z$:u:z	z (EDAX)	Oxygen (wt%)	Nitrogen (wt%)	Proposed stoichiometry	t (nm)	Cell parameter, a (Å)
0.6:0.2:0.2	0.57:0.19:0.24	1.7(1)	9.2(3)	$V_{0.6}Mo_{0.2}W_{0.2}(O_{0.1}N_{0.64})$	10	4.1373 (3)
0.4:0.4:0.2	0.42:0.37:0.21	3.6(3)	11.1(4)	$V_{0.4}Mo_{0.4}W_{0.2}(O_{0.25}N_{0.88})$	12	4.1288 (3)
0.4:0.2:0.4	0.41:0.17:0.42	3.1(3)	7.5(3)	$V_{0.4}Mo_{0.2}W_{0.4}(O_{0.24}N_{0.68})$	9	4.1415 (2)
1/3:1/3:1/3	0.34:0.34:0.32	2.6(2)	9.2(3)	$V_{1/3}Mo_{1/3}W_{1/3}(O_{0.2}N_{0.82})$	9	4.1537 (4)
0.2:0.6:0.2	0.2:0.62:0.18	2.1(2)	9.8(3)	$V_{0.2}Mo_{0.6}W_{0.2}(O_{0.16}N_{0.83})$	10	4.1532 (2)
0.2:0.4:0.4	0.2:0.39:0.41	5.3(2)	8.3(3)	$V_{0.2}Mo_{0.4}W_{0.4}(O_{0.47}N_{0.83})$	9	4.1586 (2)
0.2:0.2:0.6	0.18:0.2:0.62	1.8(1)	9.6(3)	$V_{0.2}Mo_{0.2}W_{0.6}(O_{0.18}N_{1.08})$	10	4.1740 (2)

$2\theta 30-70^\circ$ with a collection time of 5 s per step. The cell parameters of each product were obtained by profile fitting of the pattern using the Le Bail's method [18] as implemented in the FULLPROF program [19], from patterns collected with a scanning step of 0.02° in 2θ, over a wider angular range ($2\theta 20-120^\circ$), and with a longer acquisition time (10 s per step) in order to enhance statistics. The fits were performed using a pseudo-Voigt peak-shape function. In the final runs, usual profile parameters (scale factors, background coefficients, zero-points, half-width, pseudo-Voigt and asymmetry parameters for the peak-shape) were refined. All graphical representations relating to X-ray powder diffraction patterns were performed using the DRXWin [20] and WinPLOTR [21] programs.

2.2.3. Microstructural characterization

The morphology of all the freeze dried, crystalline precursors and the resulting oxynitrides was observed using a scanning electron microscope (Hitachi S-4100) operating at an accelerating voltage of 30 kV. All the preparations were covered with a thin film of gold for better image definition.

2.2.4. Magnetic characterization

Magnetization and alternating current (ac) susceptibility measurements were performed in a Quantum Design superconducting quantum interference device magnetometer. The magnetization measurements were performed at 1 T in the temperature range 2–100 K. Transition temperatures (T_c) were determined by ac susceptibility measurements performed in the temperature range 1.8–10 K, and frequency and exciting field of 333 Hz and 1 Oe, respectively.

3. Results

Rock salt-type interstitial (with N atoms occupying octahedral sites) crystalline phases, which are tolerant to

a certain non-stoichiometry range, have been characterized in each one of the individual V–N, Cr–N, Mo–N and W–N systems. Indeed, the respective compositions for the cubic nitride phases have been given as δ-VN_{1-x} ($0 \leqslant x \leqslant 0.15-0.2$), δ-CrN_{1-x} (with a narrow range of x values), γ-Mo_2N_{1+x} ($-0.2 \leqslant x \leqslant 0.3$) and W_2N [22]. In addition, hexagonal interstitial crystalline phases also have been characterized in these binary systems, with compositions β-V_2N, ε-Cr_2N, δ-MoN and δ-WN (and different homogeneity ranges) [23].

As mentioned in Section 1, we previously reported on the existence of the solid solutions $V_{1-z}Mo_z(O_xN_y)$, $V_{1-z}Cr_z(O_xN_y)$ and $Cr_{1-z}Mo_z(O_xN_y)$ ($0 \leqslant z \leqslant 1$), based on a fcc array of the metal atoms [13,14]. Our success in the preparation of these series was based on the careful control of the experimental conditions appropriate to the preparation of rock salt-type single-phase samples. In the present work, we have extended our synthetic approach to the synthesis of polymetallic W-containing rock salt-type oxynitrides. So, our first goal in this work was to investigate the optimal conditions for obtaining the W-only containing cubic phase with our experimental array when starting from amorphous precursors. We have used long reaction times (12 h, to eliminate time as variable) and temperatures ranging from 673 to 1173 K. In this way, it was possible to evaluate also the influence of the cooling rate, another variable that sometimes is key in this type of processes [16]. Fig. 1 shows the X-ray diffraction patterns of the products resulting from the ammonolysis processes when subjected to fast cooling rate after treatment at the indicated temperature. As can be noted, the cubic phase (JCPDS Card 25-1257) is obtained at temperatures as low as 873 K. At lower temperatures ($\leqslant$673 K), WO_2 is obtained (JCPDS Card 32-1393). The cubic phase is obtained pure only in the temperature range 873–973 K. At 1073 K, the majority phase is W metal (JCPDS Card 04-0806) and, at 1173 K, the cubic phase is practically absent. These results are practically independent on the cooling rate. The only difference is that, with a slow cooling rate, the intensity of the cubic phase peaks referred to the W ones is higher, this indicating that W metal ammonolysis occurs at low temperatures.

In the Mo–W system, we have selected, from the above, an ammonolysis temperature between 973 and 1023 K, depending on composition, after 2 h of thermal treatment, as adopted conditions for the preparation of compounds in the $Mo_{1-z}W_z(O_xN_y)$ series. We have used slow cooling rates in all samples except in the Mo-only containing one, in which quenching is required for obtaining the cubic phase [13]. Under these conditions, all compositions ($0 \leqslant z \leqslant 1$) in this series are prepared as single phases.

When the same experimental procedure is applied for obtaining compounds in the $V_{1-z}W_z(O_xN_y)$ series, one observes a certain amount of W metal together with the respective bimetallic oxynitride phase. The variation of the synthetic conditions (temperature, reaction time, cooling rate) does not lead to single phases. So, we decided to explore the use of crystalline precursors. In this case, we have found that their ammonolysis at 1073 K during 2 h with slow cooling rates allows the preparation of single phases.

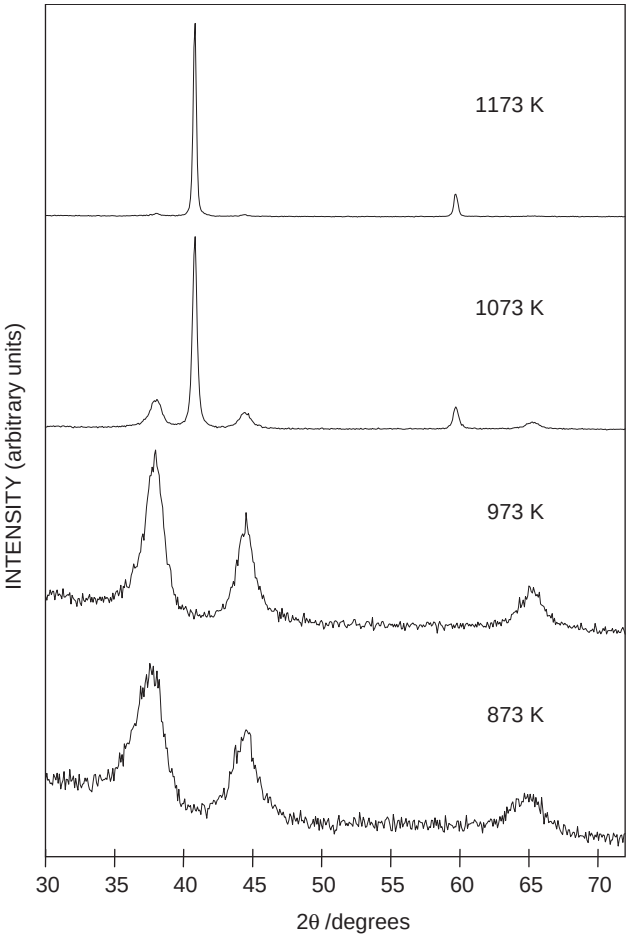

Fig. 1. X-ray diffraction patterns of the products resulting from ammonolysis of the freeze-dried precursor containing only tungsten at different temperatures, for 12 h of thermal treatment and fast cooling rates. The pattern at 1173 K corresponds to W.

In the V–Mo–W system, the use of amorphous precursors always leads to the presence of W metal as impurity together with the cubic oxynitride. However, as in the V–W system, ammonolysis of crystalline precursors at 1073 K, during 2 h with slow cooling rates, leads to single phases.

Figs. 2–4 show X-ray diffraction patterns corresponding to samples of different compositions in the series $Mo_{1-z}W_z(O_xN_y)$ and $V_{1-z}W_z(O_xN_y)$ ($z = 0$, 0.2, 0.4, 0.5, 0.6, 0.8, 1), and $V_{1-u-z}Mo_uW_z(O_xN_y)$ (u, $z = 0.2$, 0.33, 0.4, 0.6; $u + z < 1$) prepared by ammonolysis of the appropriate precursors under the above established conditions. The patterns are characteristic of a rock-

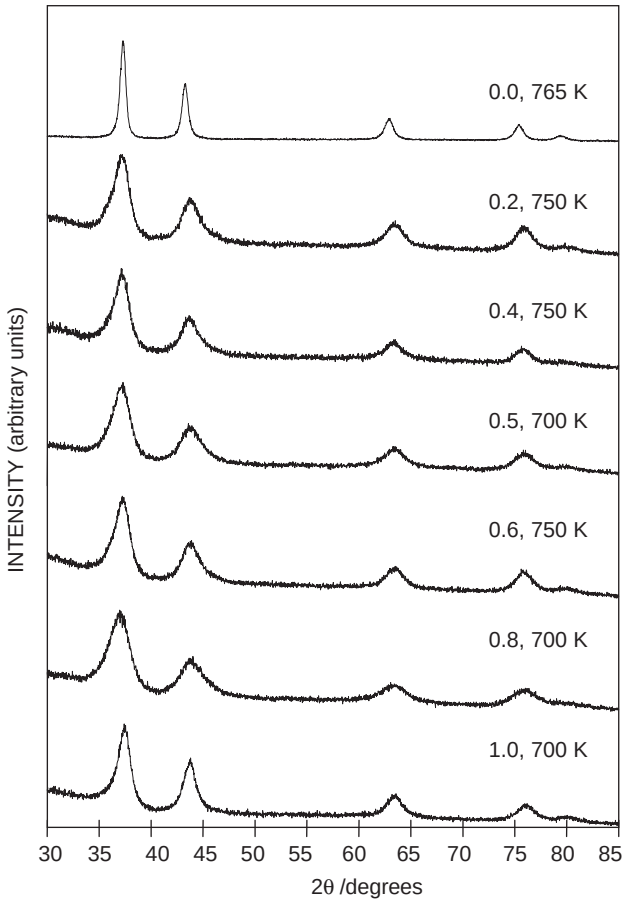

Fig. 2. X-ray diffraction patterns of $Mo_{1-z}W_z(O_xN_y)$ materials prepared by ammonolysis of freeze-dried precursors.

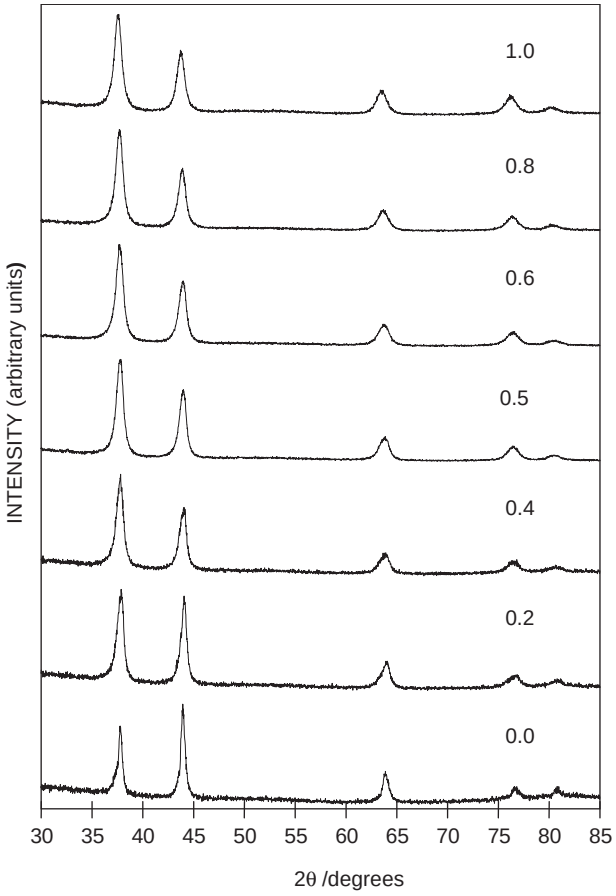

Fig. 3. X-ray diffraction patterns of $V_{1-z}W_z(O_xN_y)$ materials prepared by ammonolysis of crystalline precursors.

salt structure, and the cell parameters have been calculated by profile fitting of the patterns, using the method of LeBail as implemented in the FULLPROF program (Tables 1–3). The cell dimensions of the synthesized oxynitrides fit in well with those previously reported for related phases.

Tables 1–3 show the results of the chemical analysis of the resulting products (black powders). In all cases, the Mo:W, V:W, or V:Mo:W ratios are (within experimental error) equal to the nominal value in the corresponding precursor. The nitrogen content was determined from standard combustion analyses, whereas the oxygen content was indirectly estimated by thermogravimetric analysis. The TGA profiles indicate that oxidation of the bulk samples occurs in a one step process (ranging from 573–673 to 723–773 K, depending on the oxynitride composition). The final products are mixtures of V_2O_5, MoO_3 and WO_3. Low temperature oxidation is consistent with the pyrophoric character of these products, what makes passivation necessary.

Figs. 5–7 show characteristic SEM images corresponding to representative samples in the $Mo_{1-z}W_z(O_xN_y)$, $V_{1-z}W_z(O_xN_y)$ and $V_{1-u-z}Mo_uW_z(O_xN_y)$ series. In the Mo–W system, the freeze-dried precursor is comprised of very large sheets with a typical width of 2–5 μm. In turn, these large sheets consist of fine sheets with typical dimensions $300 \times 300 \times 30$ nm (Figs. 5a). The external appearance of the large sheets remains practically unchanged during the ammonolysis process yielding $Mo_{1-z}W_z(O_xN_y)$, but the fine structure is lost and the resulting large sheets show now wrinkled surfaces. In fact, SEM images at high magnification clearly reveal that $Mo_{1-z}W_z(O_xN_y)$ grains are aggregates of nanometer spherical particles with typical diameter around 10 nm (Fig. 5b). In the V–W system, the crystalline precursor is formed by a mixture of large sheets of WO_3 surrounded by spherical particles of V_2O_5 (Fig. 6a). The corresponding oxynitrides obtained by ammonolysis of crystalline precursors consists in spherical particles of typical diameter around 150 nm that present wrinkled surfaces. SEM images at high magnification show that $V_{1-z}W_z(O_xN_y)$ grains are aggregates of nanometer spherical particles with typical diameter around 15 nm (Fig. 6b). Finally, in the V–Mo–W system, the crystalline precursor consists of large and rectangular sheets (Fig. 7a), and the corresponding oxynitrides maintain this array, except by the fact that the sheets present now a wrinkled surface. SEM images

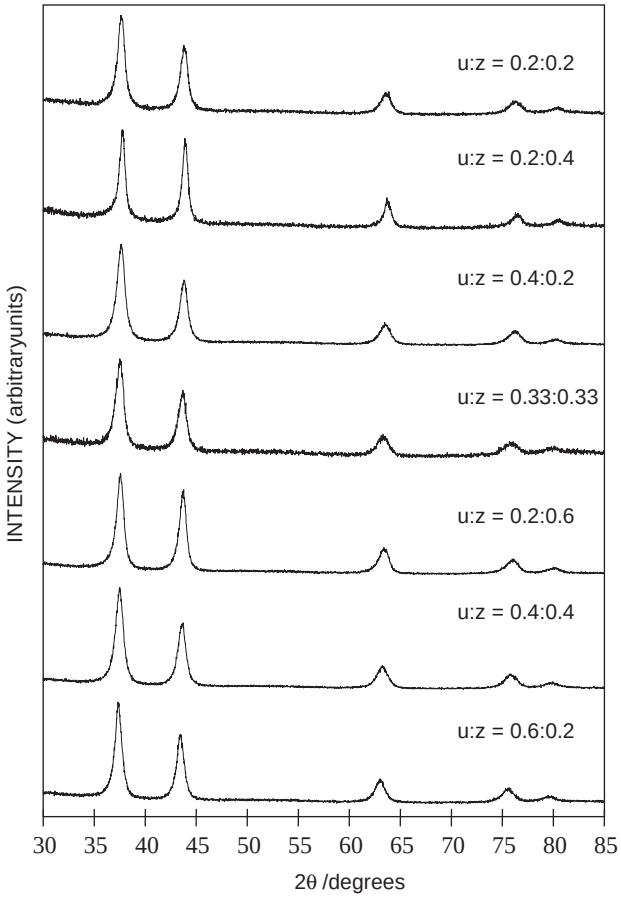

Fig. 4. X-ray diffraction patterns of $V_{1-u-z}Mo_uW_z(O_xN_y)$ materials prepared by ammonolysis of crystalline precursors.

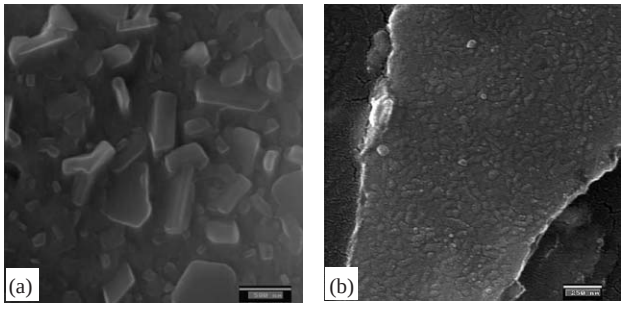

Fig. 5. SEM images showing the microstructure of the amorphous precursor (a) and the oxynitride (b) in the $Mo_{1-z}W_z(O_xN_y)$ series. Scale bars corresponds to 500 and 250 nm, respectively.

at high magnification show that the grains are aggregates of nanometer spherical particles with typical diameter around 10 nm (Fig. 7b).

The size of the crystallites (Tables 1–3) has been calculated from the XRD patterns (by a standard Scherrer analysis of the half-width of the XRD peaks, following the method described in Ref. [23]). Well crystallized $Pb(NO_3)_2$ was used as standard to calibrate the intrinsic width associated to the equipment. Crystal-

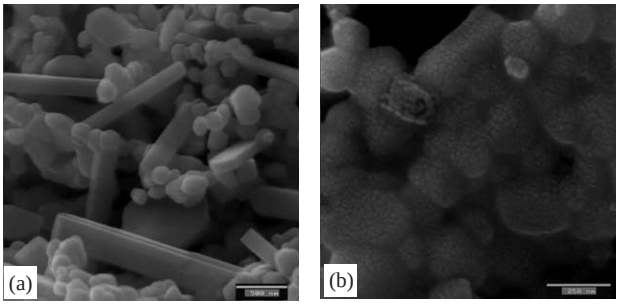

Fig. 6. SEM images showing the microstructure of the crystalline precursor (a) and the oxynitride (b) in the $V_{1-z}W_z(O_xN_y)$ series. Scale bars corresponds to 500 and 250 nm, respectively.

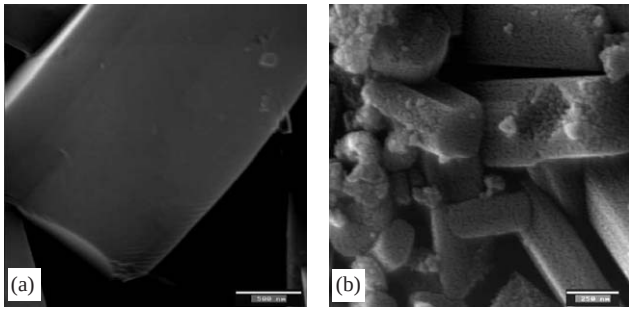

Fig. 7. SEM images showing the microstructure of the crystalline precursor (a) and the oxynitride (b) in the $V_{1-u-z}Mo_uW_z(O_xN_y)$ series. Scale bars corresponds to 500 and 250 nm, respectively.

lite size remains practically constant in the three series (ca. 5 nm for $Mo_{1-z}W_z(O_xN_y)$, and 10 nm for $V_{1-u-z}Mo_uW_z(O_xN_y)$ and $V_{1-z}W_z(O_xN_y)$).

Fig. 8 shows the temperature dependence of both the in-phase, χ', and the out-of-phase, χ'', components of the ac susceptibility for the $Mo_{1-z}W_z(O_xN_y)$ samples with $z = 0$ and 0.5. In both cases, one feature is clearly distinguishable in the χ' variation, corresponding to an abrupt drop, which reach negative values. This feature defines the critical temperature, T_c, for the transition from normal to superconducting state in these samples. In addition, associated with the drop in χ', the appearance of magnetic energy absorption is detected as a sudden increase in χ''. This behaviour is typical of a single superconducting phase. Due to the low values of T_c, the regime of total shielding due to induced currents is not established. The corresponding T_c values are 5.0 and 2.6 K. In this series, the samples with $z = 0.2$, 0.4 and 0.6 also are superconducting ($T_c = 2.6$ K, in all cases), although the experimental χ' values are significantly lower than those presented in Fig. 8. On the other hand, in the $V_{1-z}W_z(O_xN_y)$ series, only the sample with $z = 0$ is superconducting (T_c 7.5 K), but also with very low values of χ'. In contrast, when magnetization measurements were performed in a magnetic field of 1000 Oe, the superconducting transition only was observed for the $Mo(O_xN_y)$ sample.

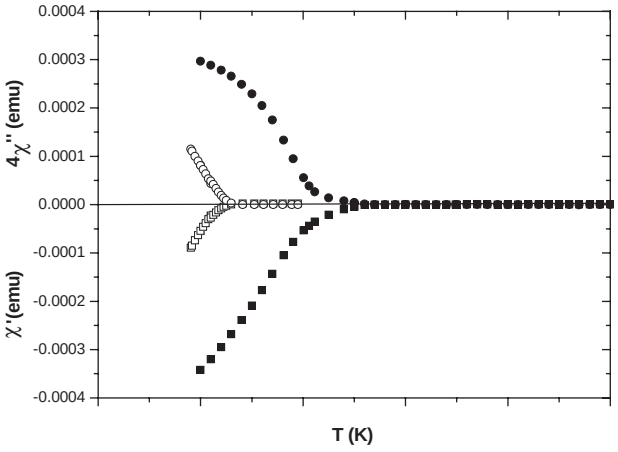

Fig. 8. In-phase, χ' (circles) and out of phase, χ'' (squares) components of the ac susceptibility of samples $Mo_{1-z}W_z(O_xN_y)$ with $z = 0.00$ (closed symbols) and 0.50 (open symbols).

4. Discussion

As stated above, an objective of the present work was to expand the application of a preparative technique that has proved its versatility for obtaining a diversity of complex polymetallic systems of interest. In turn, as more comparative results are available, we can discuss in more detail about the reliability of the technique.

An interesting result of our previous work on bimetallic Mo-containing (and V or Cr) oxynitrides [13,14] was the observation that the non-metal (N and/or O) to metal molar ratio approaches 1 in the Mo-rich samples. It seems that, in the presence of oxygen, the fcc array of the metal atoms becomes stabilized respect to the hexagonal phase for the Mo-rich samples, and the N and O atoms occupy all the octahedral interstitial positions. In fact, Oyama et al. also noted such a stabilization of the cubic phase when studying bimetallic oxynitrides of V, Mo, W and Nb [16]. Results in the present work point in the same sense: for Mo and/or W rich samples, the compounds have the rock-salt crystal structure, with a non-metal to metal content around 1. We can conclude that the fcc array of the metal atoms with all the octahedral positions occupied by N or O atoms becomes stabilized in the Mo and W bimetallic oxynitrides, in contrast to that observed for the corresponding single (Mo or W) nitride phases.

One aspect that deserves some explanation is that concerning the proposed nitrogen and oxygen stoichiometry. Samples in these solid solution series tend to be pyrophoric, which is the reason for what they must be passivated (treatment under N_2 atmosphere) prior to their manipulation. The purpose of this passivation is to cover the active surface of the material with a layer of oxide (O_2 present as impurity in N_2) to prevent oxidation of the bulk. Thus, besides the incorporation of oxygen atoms to interstitial positions, which is determinant for stabilizing the cubic structure, surface oxidation should be the main responsible for the high non-metal content that is observed in some products. In fact, Oyama et al. also noticed the dependence of the non-metal content on procedural variables [16]. In practice, they reported very important deviations (from 1) of the non-metal to metal ratio (with values between 1.5 and 2.25), a result that could be attributed to the atmosphere (0.5% O_2–99.5% He) under which passivation was performed [16].

From the above results, we could conclude that the use of precursors really offers the advantage of a quasi-atomic level mixing of the metals in the precursors, what would decrease the diffusion distances in the subsequent reactions. This does not mean, however, that decomposition of the precursors directly leads to the desired material (i.e. without intermediates formation), what is an extended and erroneous idea. In fact, we have observed the apparition of intermediate phases (in the course of the reaction from the precursor to the bimetallic oxide) even in cases in which we have used a crystalline bimetallic precursor. Thus, in the thermal decomposition of the calcium–copper formiate, $CaCu(HCCO)_4$, the presence of nanometric CuO and CaO is detected (at 573 and 823 K, respectively) prior to the formation of $Ca_{1-x}CuO_2$ (898 K) [24]. Also, when using freeze-dried precursors for obtaining polymetallic oxides, we have observed that the reaction pathway results more or less complicated, depending on the involved metals.

Which is, then, the advantage of using freeze-dried or other precursors? Well, the characteristic low temperature decomposition of these precursors usually allows obtaining intimate mixtures of very low sized oxide particles. The reactivity of these mixtures relative to a mechanical (mixing and grinding) mixture of oxides is very high, due to two main reasons. In the mechanical mixtures, the oxide particles are aged. In this context, it must be understood as if they had suffered surface modifications that introduce kinetic barriers for subsequent reactions. Also, the particle size in mechanical mixtures is well above 1 μm, whereas in the precursor-derived mixture is around or below 100–200 nm. This represents a reduction of, at least, one order of magnitude in the diffusion lengths.

The situation, although more complicated, is similar when the route to the final product involves, after reduction of the precursor, a nitridation or carbidation process. Indeed, as far as the freeze-dried precursor has been prepared in an oxidic environment, its decomposition at low temperatures, even under a reducing atmosphere, leads to a mixture of oxides. For example, in our recent work on the synthesis of intermetallic compounds by direct reduction of freeze-dried precursors [12], we observed that the reaction from the precursor to the intermetallic

compound Co_7Mo_6 passes through mixtures of (a) Co_3Mo and $Co_2Mo_3O_8$ (between 973 and 1023 K); (b) MoO_2, Co_3Mo and Co_2MoO_3 (between 1023 and 1073 K); and (c) Co_7Mo_6, MoO_2 and Co_3Mo (between 1073 and 1123 K). Finally, Co_7Mo_6 is obtained as single-phase above 1123 K. If a subsequent nitridation or carbidation process is involved, the situation gets more complicated. In the preparation of the V and W-containing oxynitrides, we have observed that direct ammonolysis of the freeze-dried precursors, which are homogeneous at micron scale (as shown by EDAX), results in the presence of W metal in all the experimental conditions explored in this work. We consequently decided to obtain crystalline precursors. It is the ammonolysis of these crystalline precursors that leads to single-phased cubic products, without the presence of W metal. The kinetic of the reduction/nitruration processes of the highly reactive amorphous precursors leads to the formation, at low temperatures, of W metal, which is unreactive. However, the use of a less-reactive crystalline precursor avoids W formation and leads to the cubic phase. The crystalline precursors are not homogeneous, and the crystal sizes are around 150 nm. In any case, the resulting fresh mixtures of WO_3 and V_2O_5 (and MoO_3 in the trimetallic compounds) continue being more reactive than the homologous mechanical mixtures, and the diffusion lengths are, at least, one order of magnitude lower.

Finally, we must briefly refer to the magnetic behavior of these samples. As exposed above, only in the case of the $Mo(O_xN_y)$ sample, we have observed the superconducting transition both by magnetization and ac susceptibility measurements; in the remaining cases in which the superconducting transition is observed by ac susceptibility measurements, it was not observed by magnetization experiments. It must be stressed that these samples are constituted by nanoparticles whose typical size is around 10 nm. In consequence, continuous magnetic fields as low as 1000 Oe can be sufficient to destroy the superconducting state in these nanoparticles, as it happens. On the other hand, the stoichiometric variations along these series indicate that there must be a substantial degree of disorder (introduced by the presence of oxide and nitride ions at random) in the lattice, and disorder is a parameter that strongly affects superconductivity. We think that this is the reason why the $Mo_{1-z}W_z(O_xN_y)$ samples with $x = 0.20$, 0.40, 0.50 and 0.60 present the same apparent critical temperature. Even we do not discard a small (but variable) amount of a superconductor impurity phase of fixed composition with a certain $T_c = 2.6$ K.

In conclusion, we have prepared new interstitial molybdenum–tungsten, vanadium–tungsten and vanadium–molybdenum–tungsten oxynitrides in the solid solution series $Mo_{1-z}W_z(O_xN_y)$ and $V_{1-z}W_z(O_xN_y)$ ($z = 0.0$, 0.2, 0.4, 0.5, 0.6, 0.8, 1.0), and $V_{1-u-z}Mo_uW_z(O_xN_y)$ (u, $z = 0.2$, 0.33, 0.4, 0.6; $u + z < 1$), verifying the versatility of a relatively simple processing route to complex ad hoc compositions.

Acknowledgments

This research was supported by the Spanish Ministerio de Ciencia y Tecnología (MAT96-1037, PB98-1424, MAT2002-03803, MAT 2003-01696, MAT2001-3334 and 1FD97-1422-MAT). The SCSIE of the University of Valencia and the SEGAI of the University of La Laguna are acknowledged for X-ray diffraction, microscopy and analytical facilities. One of us (A.E.) wish to thank to Agencia Española de Cooperación Internacional (AECI) for financial support.

References

[1] F.J. Disalvo, Science 247 (1990) 649–655.
[2] (a) H.J. Goldschmidt, Interstitial Alloys, Plenum Press, New York, 1967, pp. 214–244;
(b) L.E. Toth, Transition Metal Carbides and Nitrides, Academic Press, New York, 1971;
(c) R.B. Levy, M. Boudart, Science 181 (1973) 547;
(d) L. Volpe, M. Boudart, Catal. Rev. Sci. Eng. 27 (1985) 515;
(e) L. Volpe, M. Boudart, J. Solid State Chem. 59 (1985) 332;
(f) J.F. Shakelford, Introduction to Materials Science for Engineers, Macmillan, New York, 1988;
(g) T.S. Oyama, J. Solid State Chem. 96 (1992) 442;
(h) E.L. Kugle, L.E. McCandlish, A.J. Jacobson, R.R. Chianelli, US Patent 5 138 111, 1992.
[3] D.R. Glasson, S.A. Jayaweera, J. Appl. Chem. 18 (1968) 65.
[4] R. Niewa, F.J. DiSalvo, Chem. Mater. 10 (1998) 2733.
[5] D.H. Gregory, J. Chem. Soc. Dalton Trans. 3 (1999) 259.
[6] S.T. Oyama (Ed.), The Chemistry of Transition Metal Carbides and Nitrides, Blackie Academic & Professional, Chapman & Hall, London, 1996;
Y. Laurent, P. Verdier, International Symposium on Nitrides, J. Eur. Ceram. Soc. 17 (1997) 1773–2037.
[7] S. Alconchel, F. Sapiña, D. Beltrán, A. Beltrán, J. Mater. Chem. 9 (1999) 749.
[8] (a) S.H. Elder, L.H. Doerrer, F.J. DiSalvo, J.B. Parise, D. Gouyomard, J.M. Tarascon, Chem. Mater. 4 (1992) 928;
(b) D.S. Bem, H.C. zur Loye, J. Solid State Chem. 104 (1993) 467;
(c) J.D. Houmes, D.S. Bem, H.-C. zur Loye, in: A.R. Barron, G.S. Fischman, M.A. Fury, A.F. Hepp (Eds.), MRS Symposium Proceedings: Covalent Ceramics II: Non-Oxides, Vol. 327, Materials Research Society, Boston, MA, 1993, p. 153;
(d) D.S. Bem, C.P. Gibson, H.-C. zur Loye, Chem. Mater. 5 (1993) 397;
(e) D.S. Bem, H.P. Olsen, H.-C. zur Loye, Chem. Mater. 7 (1995) 1824;
(f) P. Herle Subramanya, N.Y. Vasanthacharya, M.S. Hedge, J. Gopalakrishnan, J. Alloys Compds. 217 (1995) 22;
(g) D.S. Bem, C.M. Lampe-Onnerud, H.P. Olsen, H.-C. zur Loye, Inorg. Chem. 35 (1996) 581;
(h) R.N. Panda, N.S. Gajbhiye, J. Alloys Compds. 256 (1997) 102.

[9] (a) K.S. Weil, P.N. Kumta, Mater. Sci. Eng. B38 (1996) 109;
(b) K.S. Weil, P.N. Kumta, J. Solid State Chem. 128 (1997) 185;
(c) K.S. Weil, P.N. Kumta, J. Solid State Chem. 134 (1997) 302;
(d) K.S. Weil, P.N. Kumta, Acta Crystallogr. C 53 (1997) 1745;
(e) P. Herle Subramanya, M.S. Hedge, K. Sooryanarayana, T.N. Guru Row, G.N. Subbanna, J. Mater. Chem. 8 (1998) 1435.
[10] V. Primo, F. Sapiña, M.J. Sanchis, R. Ibañez, D. Beltrán, A. Beltrán, Solid State Ion. 872 (1993) 63–65.
[11] A. El-Himri, F. Sapiña, R. Ibañez, A. Beltrán, J. Mater. Chem. 11 (2001) 2311 and references therein.
[12] D. Vie, N. Valero, E. Martínez, F. Sapiña, J.V. Folgado, A. Beltrán, J. Mater. Chem. 12 (2002) 1017–1021.
[13] A. El-Himri, M. Cairols, S. Alconchel, F. Sapiña, R. Ibañez, D. Beltrán, A. Beltrán, J. Mater. Chem. 9 (1999) 3167.
[14] A. El-Himri, F. Sapiña, R. Ibañez, A. Beltrán, J. Mater. Chem. 10 (2000) 2537.
[15] S.T. Oyama, R. Kieffer, in: M. Howe-Grant (Ed.), Kirk–Othmer Encyclopedia of Chemical Technology, 4th Edition, Wiley, New York, 1992, p. 841.
[16] (a) C.C. Yu, S. Ramanathan, F. Sherif, S.T. Oyama, J. Phys. Chem. 98 (1994) 13038;
(b) C.C. Yu, S.T. Oyama, J. Solid State Chem. 116 (1995) 205;
(c) C.C. Yu, S.T. Oyama, J. Mater. Sci. 30 (1995) 4037;
(d) R. Kapoor, S.T. Oyama, B. Frühberger, J.G. Chen, J. Phys. Chem. B 101 (1997) 1543;
(e) C.C. Yu, S. Ramanathan, S.T. Oyama, J. Catal. 173 (1998) 1;
(f) S. Ramanathan, C.C. Yu, S.T. Oyama, J. Catal. 173 (1998) 10;
(g) S.T. Oyama, C.C. Yu, F.G. Sherif, US Patent 5 444 173, 1995.
[17] S.T. Oyama, Catal. Today 15 (1992) 179; C.J.H. Jacobsen, Chem. Commun. (2000) 1057.
[18] A. Le Bail, H. Duroy, J.L. Fourquet, Mater. Res. Bull. 23 (1988) 447.
[19] J. Rodriguez-Carvajal, FULLPROF Program, in: Collected Abstracts of Powder Diffraction Meetting, Toulouse, France, 1990, pp. 127–128.
[20] V. Primo, Powder Diffrac. 14 (1999) 70.
[21] J. Rodríguez-Carvajal, T. Roisnel, FullProf.98 and WinPLOTR: New Windows 95/NT Applications for Diffraction, Newsletter, 20, (May–August) (1998).
[22] P. Ettmayer, W. Lengauer, in: R. Bruce King (Ed.), Encyclopedia of Inorganic Chemistry, Wiley, Chichester, 1994, p. 2498.
[23] R. West, Solid State Chemistry and its Applications, Wiley, Chichester, 1984, pp. 173–175.
[24] (a) M.J. Sanchis, F. Sapiña, R. Ibañez, A. Beltrán, D. Beltrán, Mater. Lett. 12 (1992) 409;
(b) M.J. Sanchis, M. Burgos, R. Carrasco, F. Sapiña, R. Ibañez, D. Beltrán, A. Beltrán, Solid State Ion. 66 (1993) 27.